Control of Patterns of Corneal Innervation by Pax6

Lucy J. Leiper,[1] *Jingxing Ou,*[1] *Petr Walczysko,*[1] *Romana Kucerova,*[1] *Derek N. Lavery,*[1] *John D. West,*[2] *and J. Martin Collinson*[1]

Purpose. Corneal nerves play essential roles in maintaining the ocular surface through provision of neurotrophic support, but genetic control of corneal innervation is poorly understood. The possibility of a neurotrophic failure in ocular surface disease associated with heterozygosity at the Pax6 locus (aniridia-related keratopathy [ARK]) was investigated.

Methods. Patterns of corneal innervation were studied during development and aging in mice with different Pax6 dosages and in chimeras. Immunohistochemistry and ELISA-based assays were used to determine the molecular basis of defects seen in Pax6 mutants, and wound healing assays were performed.

Results. In adults, the *Pax6*$^{+/-}$ epithelium was less densely innervated than the wild-type epithelium, and radial projection of epithelial nerves was disrupted. Neurotrophic support of the corneal epithelium appeared normal. Directed nerve projection correlated with patterns of epithelial cell migration in adult wild-types, but innervation defects observed in *Pax6*$^{+/-}$ mice were not fully corrected in wound healing or chimeric models where directed epithelial migration was restored.

Conclusions. Pax6 dosage nonautonomously controls robust directed radial projection of corneal neurons, and the guidance cues for growth cone guidance are not solely dependent on directed epithelial migration. There is little evidence that ARK represents neurotrophic keratitis. (*Invest Ophthalmol Vis Sci.* 2009;50:1122–1128) DOI:10.1167/iovs.08-2812

The transcription factor PAX6 is essential for eye development and is found in several ocular cell types, including the corneal and limbal epithelia, where gene expression is maintained throughout life.[1–4] Heterozygous deficiencies in *PAX6* are characterized by iris hypoplasia, corneal epithelial fragility, persistent lens-corneal bridge (Peter's anomaly) and corneal opacity, with vascularization and inflammation termed *aniridic keratopathy* or *aniridia-related keratopathy* (ARK).[5–8] Mouse *Pax6*$^{+/-}$ corneas are an excellent model of human ARK.[4,6,9–11]

The corneal epithelium is one of the most densely innervated tissues of the body and receives sensory nerve fibers that originate principally in the trigeminal ganglion.[12–14] The nerve bundles enter the corneal periphery radially to form the perilimbal ring.[15] Bundles of fibers project and extend through the corneal stroma, subdivide, penetrate the anterior limiting lamina, and innervate the corneal epithelium, forming a basal epithelial nerve plexus.[13,14] The mechanisms that control corneal epithelial nerve growth are incompletely known, but wound-induced electric currents have been shown to direct nerve regeneration after epithelial wounding.[16]

Corneal nerves maintain a healthy cornea through the release of soluble trophic factors.[17,18] Substance P (SP) is of particular importance; it acts synergistically with other growth factors, including nerve growth factor (NGF), to accelerate corneal epithelial cell migration and proliferation during healing and regeneration.[18–27]

Disruption of corneal innervation can cause degenerative conditions ranging from dry eye to neurotrophic keratitis.[28] The symptoms accelerate cell loss leading to corneal epithelial thinning, increased epithelial permeability, and wound healing deficiency. Most neurotrophic keratitis results from herpetic viral infection; however, ocular surgery such as laser-assisted in situ keratomileusis (LASIK) and corneal transplants, even the use of contact lenses, can lead to damage of corneal nerves.[28–31] We hypothesized that corneal epithelial degeneration in *PAX6*$^{+/-}$ humans and mice may be in part a type of neurotrophic keratitis.

Methods

Mice

Pax6$^{+/Sey\text{-}Neu}$ (*Pax6*$^{+/-}$) mice[1] were maintained on the CBA/Ca genetic background by heterozygous mating. *Pax6* overexpressing transgenics, called *PAX77*,[32] were maintained on the CBA/Ca genetic background, breeding *PAX77*$^{+}$ × wild-type CBA/Ca. The H253 (*XLacZ*) transgenic line,[33] which is mosaic for *LacZ* expression from an X-linked *LacZ* reporter, was mated to *Pax6*$^{+/-}$ as described previously.[34] Experimental *Pax6*$^{+/+}$ ↔ *Pax6*$^{+/-}$, *LacZ*$^{+}$ and control *Pax6*$^{+/+}$ ↔ *Pax6*$^{+/+}$, *LacZ*$^{+}$ chimeras were produced as described previously.[34] All experiments were performed in accordance with the ARVO Statement for the Use of Animals in Ophthalmic and Vision Research.

Chemicals and Reagents

NGF, SP, and anti–β-tubulin III were from Sigma-Aldrich (Poole, Dorset, UK). Anti-TrkA was from AbCam (Cambridge, UK), and anti-TrkB and TrkC were from Santa Cruz Biotechnology (Santa Cruz, CA).

Immunohistochemistry on Whole Mount Corneas

Embryos or eyes were fixed in 4% wt/vol paraformaldehyde for 2 hours at 4°C and in methanol for 1 hour at −20°C. Dissected corneas were incubated in 1% pepsin in 10 mM HCl, 37°C, 20 minutes followed by 10-minute incubation in 0.1 M sodium borate, pH 8, at room temperature, and 3 × 20 minutes PBS. Corneas were blocked for 30 minutes (0.3% BSA, 4% normal goat serum, 0.1% Triton X-100, PBS) and incubated with anti–β-tubulin III; Tuj 1, 1:1000) overnight at 4°C. After 1 hour in PBS, secondary antibody (Alexa-Fluor 488 donkey anti-rabbit, 1:300, blocking buffer) was added for 3 hours. After a 1-hour wash in PBS, corneas were mounted.

Eyes that had been XGal-stained[35] were treated similarly, but the secondary antibody was biotin-labeled anti-rabbit (Sigma-Aldrich) di-

From the [1]School of Medical Sciences, Institute of Medical Sciences, University of Aberdeen, Foresterhill, Aberdeen, United Kingdom; and the [2]Division of Reproductive and Developmental Sciences, Genes and Development Group, University of Edinburgh, Edinburgh, United Kingdom.

Supported by Wellcome Trust Grant 068932, Tenovus Scotland Grant G04/1, and Newlife (BDF) Grant 04/07 (JMC).

Submitted for publication September 2, 2008; accepted January 19, 2009.

Disclosure: **L.J. Leiper**, None; **J. Ou**, None; **P. Walczysko**, None; **R. Kucerova**, None; **D.N. Lavery**, None; **J.D. West**, None; **J.M. Collinson**, None

The publication costs of this article were defrayed in part by page charge payment. This article must therefore be marked "*advertisement*" in accordance with 18 U.S.C. §1734 solely to indicate this fact.

Corresponding author: J. Martin Collinson, School of Medical Sciences, Institute of Medical Sciences, University of Aberdeen, Foresterhill, Aberdeen AB25 2ZD, UK; m.collinson@abdn.ac.uk.

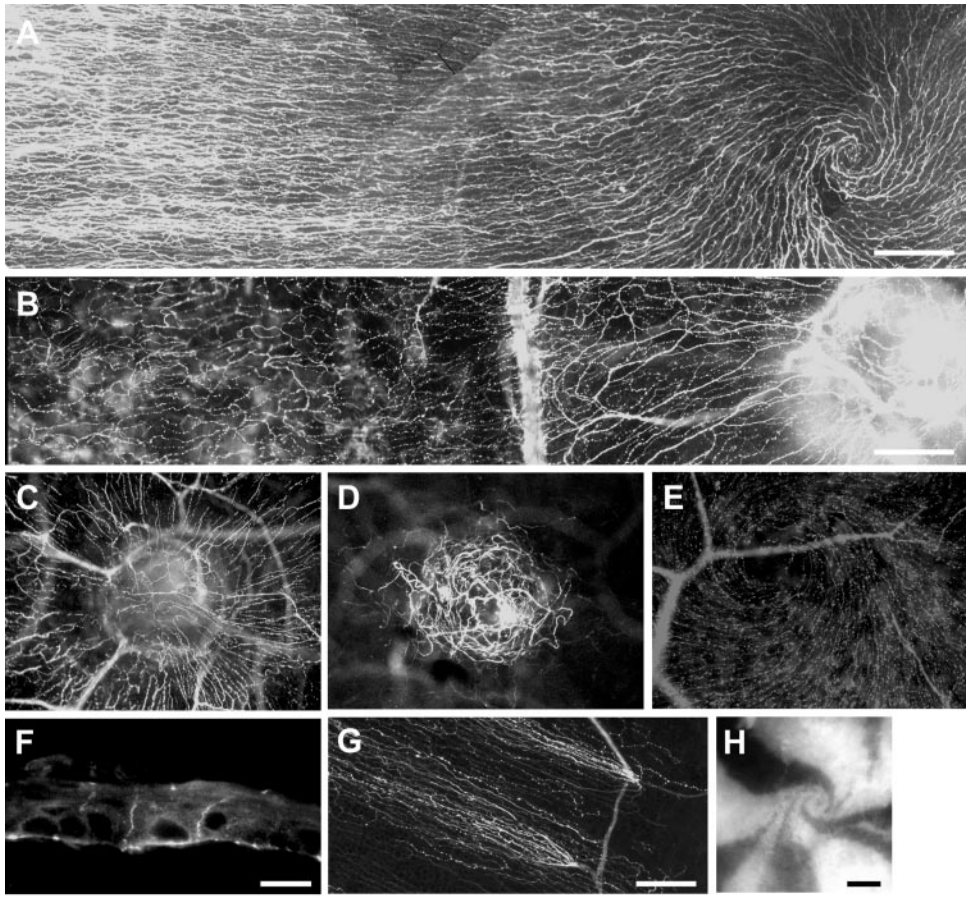

FIGURE 1. Centripetal projection of β-tubulin–expressing nerve fibers in $Pax6^{+/+}$, $Pax6^{+/-}$, and $Pax77^{+}$ mice. Anti–β-tubulin III immunofluorescence on whole mount corneas. (**A**) Centripetal projection of nerves from the limbal region to the central cornea ending in a whorl-like pattern in $Pax6^{+/+}$ corneas. (**B–D**) $Pax6^{+/-}$ corneas fibers were disorganized with radial projections disrupted in the peripheral area. Although radial projection was reestablished centrally (**B**), spiraling was absent and nerves became densely knotted on entering the lens-corneal bridge (**C**, **D**). Images of same field in superficial epithelial (**C**) and deeper stromal (**D**) planes of focus. (**E**) Normal nerve projection and central swirling in the corneal epithelium of the Pax6-overexpressing mouse of the *PAX77* line.[32] (**F**) Immunostaining of fibers was observed in basal corneal epithelium layers with projections upward to superficial cells. (**G**) Image of peripheral wild-type corneal epithelium showing radial projection (toward *top left*) of epithelial nerve fibers from underlying thick stromal bundles that are not themselves radially oriented. (**H**) Central swirl of XGal staining in corneal epithelium of $LacZ^{+} \leftrightarrow LacZ^{-}$ chimera, produced by centripetal migration epithelial cells. Part H reprinted with permission from Collinson JM, Morris L, Reid AI, et al. Clonal analysis of patterns of growth, stem cell activity, and cell movement during the development and maintenance of the murine corneal epithelium. *Dev Dyn*. 2002;224:432–440. © 2002 Wiley-Liss, Inc. Scale bars (**A**, **B**, **G**) 100 μm; (**F**) 20 μm; (**H**) 50 μm.

luted 1:300 and added to corneas for 45 minutes at room temperature. Corneas were rinsed four times in TBS for 10 minutes. Avidin/biotin ABC solution (Dako, Ely, Cambridgeshire, UK) was added for 30 minutes, and staining was visualized with diaminobenzidine.[4]

Measurement of Nerve Density and Orientation in Adult Corneas

Adult whole mount corneas were immunostained for β-tubulin III as described. For each cornea, the mean number of nerve fibers transected by 200-μm lines drawn (Photoshop; Adobe, Mountain View, CA) perpendicularly to the radius at the edge of the cornea was measured. This allowed the mean spacing of the neurites to be calculated (t). The mean spacing of fibers transected by 200-μm lines, drawn radially parallel to the neurite projection, was also measured for each cornea (r). For random orientation of nerve projections, r/t would approximate 1, whereas for radially directed nerves, $r/t > 1$.

Assay of SP Levels

SP levels in $Pax6^{+/+}$ and $Pax6^{+/-}$ were determined by ELISA immunoassay (Cayman Chemical, Ann Arbor, MI).

Wound Healing

For in vivo wound healing, mice (>8 weeks old, male and female) were anesthetized under veterinary advice. Central circular (1.5-mm diameter) corneal epithelial wounds were made, and the epithelial sheet within the wound was removed with a scalpel blade. Anesthesia was immediately reversed with the use of atipamezole hydrochloride (Antisedan, 0.014 mg/10 g subcutaneously; Pfizer Animal Health, Exton, PA) to facilitate normal blinking and tear production. Twelve hours after wounding, eyes were enucleated, fixed with paraformaldehyde, stained with Hoechst to measure the size of the wound, and immunostained with anti–β-tubulin III as described.

To assay neurotrophic modulation of healing, after wounding the eyes were enucleated and placed into serum-free media with or without SP and NGF, at 37°C, as described previously.[36]

RESULTS

Corneal Innervation in $Pax6^{+/+}$ and $Pax6^{+/-}$ Mice

The pattern of corneal neurons in the basal epithelial nerve plexus of 8- to 12-week-old $Pax6^{+/+}$ and $Pax6^{+/-}$ littermates was compared (Fig. 1). β-Tubulin III staining in flat mount wild-type corneas showed patterns of centripetal extension of axons from the limbus toward the cornea center terminating in a whorl-like pattern (Fig. 1A), in agreement with previous observations.[37] However, in the peripheral corneas of $Pax6^{+/-}$ mice, the nerves were disorganized. Radial orientation was reestablished centrally, but, on reaching the center of the $Pax6^{+/-}$ cornea, the axons become densely knotted within the basal layers of the persistent lens-corneal bridge, with no evidence of swirling (Figs. 1B-D). Centripetal projection and swirling in the *PAX77* transgenic line,[32] which overexpresses *PAX6,* was comparable to wild-type (Fig. 1E). Tissue sections confirmed that the immunostaining visualized C-fibers between the basal corneal epithelial cells (Fig. 1F). Thick nerve

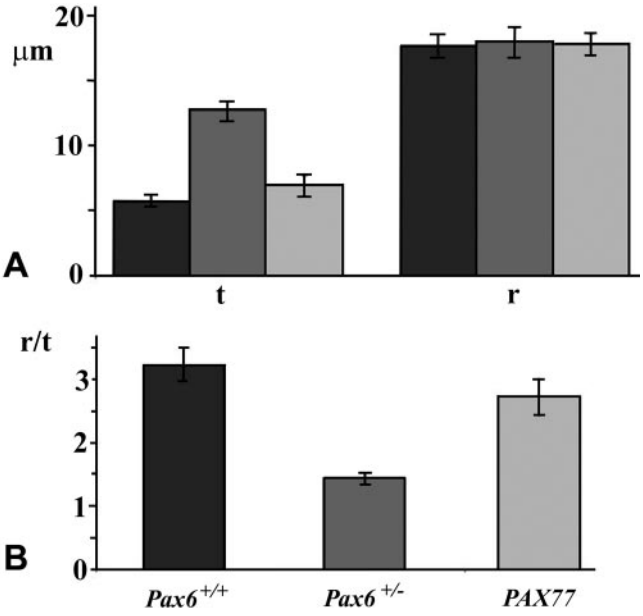

FIGURE 2. Nerve density and orientation. Nerve fiber density and orientation were measured in $Pax6^{+/+}$ (*darkest shading*), $Pax6^{+/-}$, and $PAX77^{+}$ (*lightest shading*) corneas. For each cornea the mean number of epithelial fibers was transected by 200-μm lines, drawn perpendicularly (tangential) to the radius at the edge of the cornea measured (t) giving the mean spacing of the neurites (t; **A**). Mean spacing of neurites transected by 200-μm lines, drawn radially parallel to nerve projection, was also measured for each cornea (r). For randomly oriented nerves, r/t should approximate 1. For nerves with a radially biased orientation, r/t $>$ 1 (**B**).

bundles, not necessarily radially oriented, projected through the underlying corneal stroma, penetrating the basement membrane in the peripheral cornea, from which the basal epithelial fibers directed radially (Fig. 1G). The pattern of corneal nerves in wild-type corneas was reminiscent of the patterns of centripetal epithelial cell migration observed previously (Fig. 1H).[35] The swirling patterns were maintained throughout life, although in aging mice 9 to 12 months old, significant loss of nerve terminals from sectors of the peripheral cornea was seen (18 mice; Supplementary Fig. S1, http://www.iovs.org/cgi/content/full/50/3/1122/DC1). The data showed that $Pax6^{+/-}$ corneas do have sensory nerves but that the pattern of innervation is modulated by Pax6 dosage. It was further hypothesized that nerve direction is controlled by epithelial migration.

Immunostaining of corneas from embryonic and neonatal mice showed that the radial patterns of innervation developed between postnatal day (P) 10 and P25 (Supplementary File, http://www.iovs.org/cgi/content/full/50/3/1122/DC1).

Fiber Density and Orientation

Fiber density and orientation were measured in $Pax6^{+/+}$, $Pax6^{+/-}$, and $PAX77^{+}$ corneas, as described in Methods. Briefly, the radial (r) and tangential (t) spacing of epithelial nerves within 200 μm of the edge of each cornea were measured, and an r/t ratio was calculated. For randomly oriented fibers, r/t should approximate 1. For fibers with a radially biased orientation, r/t $>$ 1. For $Pax6^{+/-}$ corneas, the tangential spacing between axons was significantly greater than for wild-type, confirming that the heterozygous cornea was less densely innervated (Fig. 2A). Spacing between the nerves in $PAX77^{+}$ corneas (mean, 6.88 μm) was not significantly different from that in wild-type corneas (mean, 5.67 μm; see Fig. 2A). The mean corneal diameter of $PAX77^{+}$ adults measures only approximately 1.5 mm, compared with 3.5 mm in wild-type adults,[36] indicating that $PAX77^{+}$ adults have fewer axons entering a significantly smaller cornea.

The r/t value for $Pax6^{+/-}$ nerves (1.43 $\pm$ 0.087 [mean $\pm$ SEM], n = 9) was significantly less than that for $Pax6^{+/+}$ or $PAX77^{+}$ (3.23 $\pm$ 0.265, n = 11; 2.72 $\pm$ 0.280, n = 10, respectively; t-test, $P < 0.005$). Hence, radial orientation of $Pax6^{+/-}$ nerves was less robust, and more random, than for $Pax6^{+/+}$ nerves. $PAX77^{+}$ corneal nerve orientation was normal (Fig. 2B).

Nerve Projection Disruption by a Lens-Corneal Bridge

The lens-corneal bridge in mice is a result of the failure of the invaginating lens placode to separate from the overlying facial epithelium.[38] We investigated whether the tangle of nerves at the center of the $Pax6^{+/-}$ cornea was a direct consequence of Pax6 mutation on projection or a secondary consequence of the presence of the lens-corneal bridge. The Pax6 null mutation was bred onto a mixed CBA/Ca $\times$ C57BL/6 background, which, though it shares all the other characteristics as the CBA/Ca $Pax6^{+/-}$ mouse, lacks the lens-corneal bridge.[39] On this background, r/t ratios (calculated as before) were 3.70 $\pm$ 0.22 (n = 12) for wild-type corneas and 2.55 $\pm$ 0.22 (n = 8) for $Pax6^{+/-}$ (t-test, P = 0.002), confirming that the less radial orientation of heterozygous nerves is robust across genetic backgrounds. Lens-corneal bridges were not present, and no neural knots were observed; rather, the nerves swirled as in wild-type corneas (n = 6; Fig. 3). It was concluded that neural knotting was a secondary consequence of the lens-corneal bridge that might have disrupted nerve guidance by acting as an attractant.

Nerve Fiber Guidance

Swirling of nerves at the center of the wild-type cornea and disrupted radial projection in the $Pax6^{+/-}$ mouse recapitulated the patterns of corneal epithelial cell migration described previously in $LacZ^{+}$ mosaics (*XLacZ*) and chimeras.[34,35] We

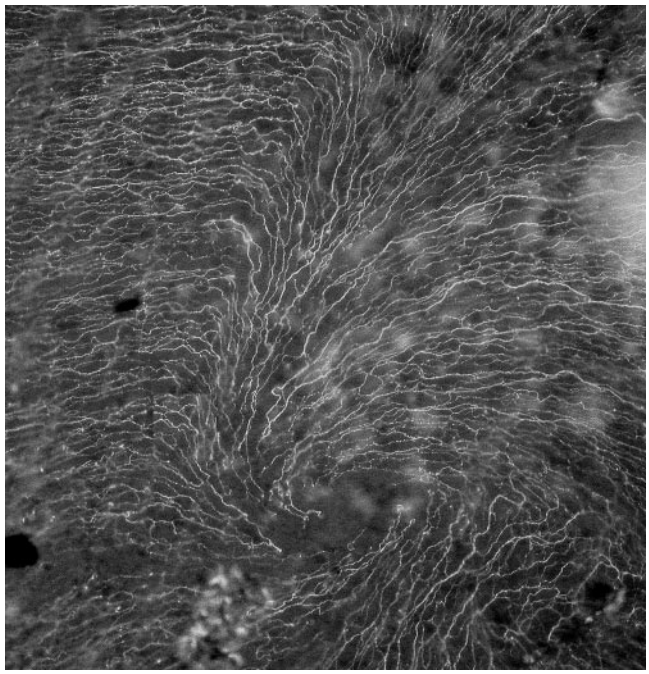

FIGURE 3. Corneal nerve projection is disrupted by the lens corneal bridge. Although radial projection is not as robust as wild-type in $Pax6^{+/-}$ cells on the mixed genetic background, normal central swirling is restored in the absence of a lens-corneal bridge.

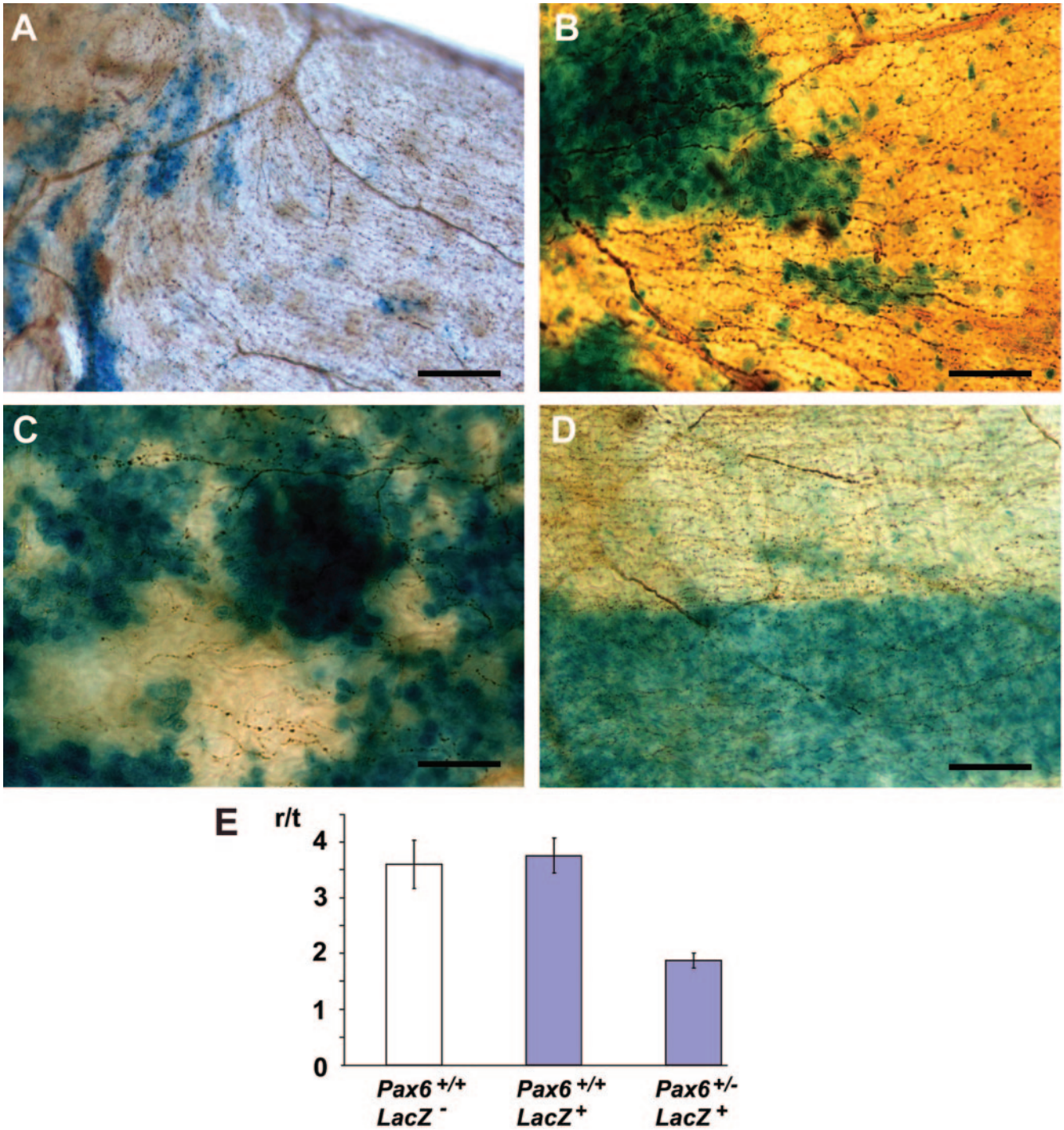

FIGURE 4. Comparison of nerve projection and epithelial cell migration. Whole mount β-tubulin immunostaining of X-Gal–stained mosaic and chimeric corneas. (**A**) Central cornea of 15-week-old $Pax6^{+/+}$ *XlacZ* mosaic. $LacZ^{+}$ epithelial cells are *blue*, epithelial nerve fibers are *brown* (β-tubulin immunostaining). Projections of the nerves lie parallel to the tracks of epithelial cell migration revealed by X-Gal staining, and there is anticlockwise swirling of both in parallel (*top left*). (**B**) Radial projection (to the left) of corneal epithelial nerve fibers across patch boundaries in a 15-week-old $Pax6^{+/-}$ *XlacZ* mosaic. (**C**) Epithelial nerves in a 3-week-old $Pax6^{+/+}$ *XlacZ* mosaic. Radial orientation of neurite projection is emerging (though not yet as regular as adults), crossing randomly oriented $LacZ^{+}$ epithelial patches. (**D**) X-Gal–stained corneal epithelium of a 15-week-old $Pax6^{+/+}$, $LacZ^{-} \leftrightarrow Pax6^{+/-}$, $LacZ^{+}$ chimera showing centripetal migration of axons. The blue stripe of epithelium is $Pax6^{+/-}$, the white is $Pax6^{+/+}$. Neurites were less dense and more randomly orientated in $Pax6^{+/-}$ blue stripes than in $Pax6^{+/+}$ white stripes. (**E**) Histogram showing r/t values for control $Pax6^{+/+}$ $LacZ^{-}$ nerves (*white bar*) compared with $Pax6^{+/+}$ $LacZ^{+}$ and $Pax6^{+/-}$ $LacZ^{+}$ (*blue bars*). Scale bars, 50 μm.

tested whether growth cone projection is dependent on directed epithelial cell migration and predicted that projection and swirling would correlate with patterns of epithelial X-Gal staining in *XLacZ* mosaic reporters. The nerves of $Pax6^{+/+}$ and $Pax6^{+/-}$ *XLacZ*-mosaic littermates were immunostained against β-tubulin III (Fig. 4). In wild-type 15-week-old corneas, nerve projections coincided with radial stripes, and there was a 1:1 correlation between the direction of epithelial swirling

(clockwise or counterclockwise) and that of the nerves (Fig. 4A; $n = 17$ [11 clockwise, 6 counterclockwise]). $Pax6^{+/-}$ $XlacZ^{+/-}$ eyes displayed disorganized clonal patterns of X-gal–stained cells, giving a patchwork appearance (Fig. 4B; $n = 8$). However, the nerves toward the center of the cornea projected radially and were able to cross clonal patches of epithelial cells. Our previous observations were that limbal stem cells and radial epithelial migration become active at 5 to 6 weeks, and in 3-week-old wild-type mice radial patterns of epithelial stripes are not yet clearly defined. However, nerves were able to project radially and to cross patches of randomly orientated blue cells in $Pax6^{+/+}$ eyes in a 3-week-old mosaic (Fig. 4C). The data suggested that corneal nerve projection does not require directed epithelial cell migration.

It remained possible that cell migration and axon guidance were responding to the same extrinsic guidance cues and that the epithelial Pax6 dosage was controlling these cues. Therefore, we produced chimeric mice to investigate whether disrupted neural patterning in the $Pax6^{+/-}$ mouse was a nonautonomous effect of reduced Pax6 dosage in the corneal epithelium (i.e., whether the genotype of the epithelium, not of the neurons, was modulating patterns of neural projection in this system). Control $Pax6^{+/+}$, $LacZ^{-} \leftrightarrow Pax6^{+/+}$, $LacZ^{+}$ and experimental $Pax6^{+/+}$, $LacZ^{-} \leftrightarrow Pax6^{+/-}$, $LacZ^{+}$ chimeras were produced as described previously.[34] In these chimeras, radial patterns of blue and white sectors were observed in the corneal epithelium that resulted from inward immigration of $LacZ^{+}$ and $LacZ^{-}$ patches of limbal-derived epithelial cells. In the control chimeras blue and white epithelial cells were $Pax6^{+/+}$, but in experimental chimeras the white cells were $Pax6^{+/+}$ and the blue cells were $Pax6^{+/-}$. The lenses in our $Pax6^{+/+} \leftrightarrow Pax6^{+/-}$ chimeras were composed entirely of wild-type cells.[40] Collinson et al.[34] showed that centripetal migration of $Pax6^{+/-}$ corneal epithelial cells was restored in $Pax6^{+/+} \leftrightarrow Pax6^{+/-}$ chimeras and that hence epithelial cell migration was, at least in part, controlled nonautonomously by cues extrinsic to the migrating cells. Nerve fibers in white, $Pax6^{+/+}$ patches of cells were on average denser and more radially oriented that those in $Pax6^{+/-}$ blue patches (Fig. 4D). Control r/t values for epithelial nerves projecting under $LacZ^{+}$ $Pax6^{+/+}$ and $LacZ^{-}$ $Pax6^{+/+}$ corneal epithelia were 3.76 ± 0.32 ($n = 9$) and 3.60 ± 0.43 ($n = 9$), respectively, showing that the presence or absence of *LacZ* does not itself affect directed migration (*t*-test; $P = 0.77$). In contrast, r/t for neurites projecting under $LacZ^{+}$ $Pax6^{+/-}$ corneal epithelial stripes was 1.88 ± 0.13 ($n = 9$), significantly less than $LacZ^{+}$ $Pax6^{+/+}$ controls (*t*-test; $P = 0.003$). Robust radial projection of epithelial neurons was, therefore, shown to be a nonautonomous function of the genotype ($Pax6^{+/+}$ or $Pax6^{+/-}$) of the corneal epithelium, and a peripheral nerve projection defect was retained even when epithelial migration was corrected.

Epithelial cells have been shown to support corneal nerves.[41–44] These data suggested that epithelial cells showed clone-specific variation in their ability to provide neurotrophic support, either in an experimental chimeric model or (in the case of aging, Supplementary Fig. S1) because of possible stochastic variation in gene expression in clones of limbal cells from which the epithelium is derived.[45] The neuropeptide SP, released by sensory neurons, has been shown to upregulate the expression of NGF by skin keratinocytes, which may in turn feed back to promote nerve survival.[46] Neurotrophic support of the cornea was investigated further.

Neurotrophic Support of the Cornea

We quantified the SP levels in $Pax6^{+/+}$ and $Pax6^{+/-}$ corneas (Fig. 5A) but found no significant difference (219.3 ± 16.95 pg/cornea and 179.3 ± 28.86 pg/cornea, respectively; *t*-test, $P > 0.05$). Although the trend was downward in $Pax6^{+/-}$ corneas, the diameter of the $Pax6^{+/-}$ cornea was approximately 90% that of wild-type on the CBA/Ca background.[40] On a per unit area basis, it can be calculated there is no deficiency of SP in the $Pax6^{+/-}$ cornea: $179.3/(0.9)^2 = 221.4$. By Western blot analysis, no difference was detected in levels of expression of NK1, the SP receptor. NGF receptors TrkA, TrkB, and TrkC were also assayed by Western blot, and all were expressed at normal levels in the $Pax6^{+/-}$ cornea (Fig. 5B).

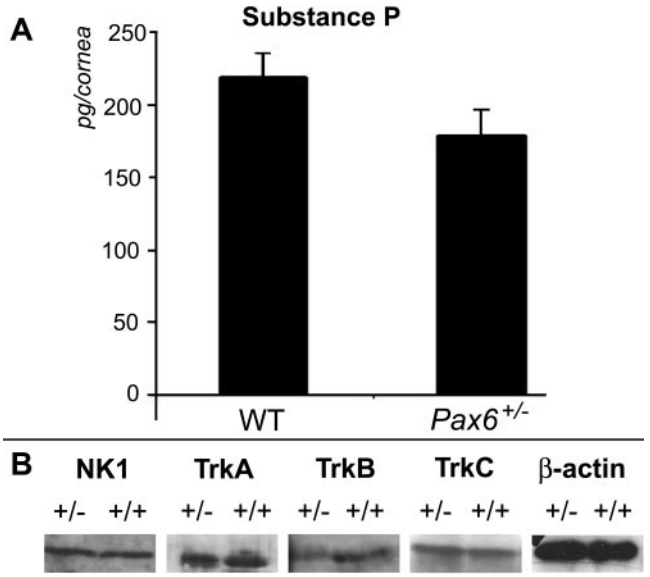

FIGURE 5. Neurotrophic support of the $Pax6^{+/-}$ cornea. (**A**) Substance P concentrations from corneal extracts derived from $Pax6^{+/+}$ and $Pax6^{+/-}$ mice, expressed as picogram per cornea. (**B**) Western blot analysis of NK1, TrkA, TrkB, and TrkC levels in $Pax6^{+/+}$ and $Pax6^{+/-}$ corneas. β-Actin was assayed as a loading control.

The effect of SP and NGF on wound closure in whole eye culture was investigated. $Pax6^{\pm}$ corneas healed slightly faster in the presence of a combination of SP and NGF (controls [mean ± SEM]: 26.3 ± 7.1 μm/h, $n = 6$; SP/NGF: 30.1 ± 5.3 μm/h, $n = 8$), but the difference was not significant (*t*-test, $P = 0.65$). NGF or SP on its own also had no significant effect. Hence, not only is SP not deficient in $Pax6^{+/-}$ corneas, adding exogenous SP does not improve epithelial performance in a wound-healing assay.

Nerve Regeneration after Wounding

In vivo epithelial wounding was performed to determine whether $Pax6^{\pm}$ corneal nerves respond normally by projecting to the wound edge in the wake of epithelial cell migration. In $Pax6^{+/+}$ and $Pax6^{+/-}$ wounds after 12 hours of healing, nerve sprouting was observed with regenerating nerves projecting usually toward the wound edge (Fig. 6). An estimate of whether the $Pax6^{+/+}$ and $Pax6^{+/-}$ nerves were equally robustly directed after wounding was obtained by measuring the tortuosity of 100 to 200 μm of each visible nerve closest to the wound edges. The straight-line distance between the growth cone (the point nearest to the wound edge) and a proximal branch point (100 to 200 μm further from the wound edge) was measured. Next the actual distance traced along the track of the nerve was measured, and this value was divided by the straight line distance to give a value of tortuosity. The tortuosity value of $Pax6^{+/-}$ nerve sprouts (1.16 ± 0.02; $n = 5$ mice, 65 nerves) was slightly but significantly greater than that of wild-type littermates (1.08 ± 0.01; $n = 6$ mice, 66 nerves; *t*-test, $P = 0.039$). Cell migration after wounding was much

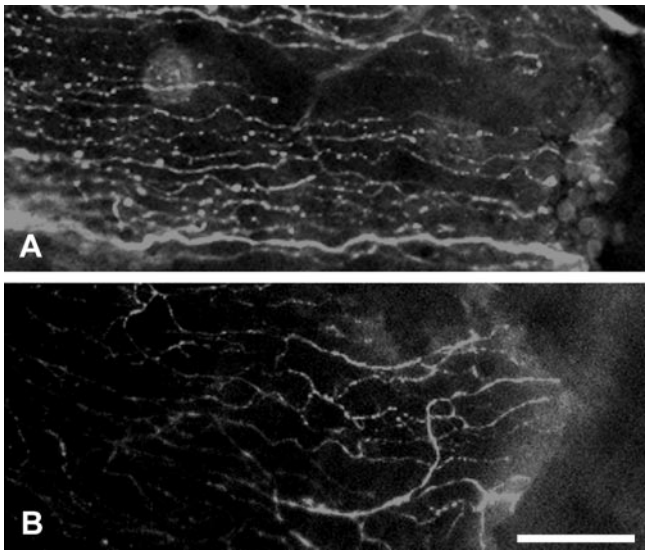

FIGURE 6. Nerve regeneration after wounding in vivo. (**A**) Representative images of a $Pax6^{+/+}$ eye stained with β-tubulin III, 12 hours after wounding, showing radial projection of regenerating nerves into the wound site (*right*). (**B**) Representative image of a β-tubulin III–stained $Pax6^{+/-}$ eye showing less robust radial nerve fiber projection toward wound (*right*). Scale bar, 50 μm.

greater (20–50 μm/h) than that observed in the uninjured corneal epithelium (20–30 μm/d).[36,47,48] Our data therefore suggested that defective $Pax6^{+/-}$ nerve projection was not corrected by the increased speed of epithelial migration.

DISCUSSION

Control of Nerve Projection in the Corneal Epithelium

Radial patterns of centripetal corneal nerve projection and swirling were observed previously in a transgenic reporter mouse and by neurotubulin staining in rats.[37,49] In vivo confocal microscopy of human corneas has revealed similar, if less regular, projections and swirls.[50,51] In the adult, there is continuous centripetal corneal epithelial cell migration, and we initially assumed that corneal nerves follow a so-called path of least resistance, swept along by the guided epithelial migration, as tentatively suggested previously.[50] The 1:1 correlation between direction of epithelial and nerve swirling at the center of the cornea is consistent with that hypothesis. However, other aspects of our data appear to preclude the possibility that nerves are directed solely by epithelial migration, as follows: the evident development of radial projection of axons in young mice before migration of epithelial cells; the radial projection of $Pax6^{+/-}$ nerves centrally in the cornea *across* randomly arranged clonal patches of epithelial cells; the retention of a quantitative guidance defect in wound healing with greatly increased rates of epithelial migration; the less robust radial projection of axons through $Pax6^{+/-}$ sectors of chimeric $Pax6^{+/+} \leftrightarrow Pax6^{+/-}$ chimeras in which patterns of normal radial epithelial cell migration have been restored. The data are more consistent with a hypothesis that epithelial cells and subepithelial nerves respond to the same external guidance cues on slightly different timescales. These cues may be electrical.

Electrical cues (ion flow) may control epithelial migration and growth cone guidance in the cornea.[16,52,53] Vertebrate-stratified epithelia, including the corneal epithelium, exhibit a net influx of sodium and potassium ions through cellular transport, combined with a net efflux of chloride ions such that basal epithelial cells are at a positive potential difference (approximately 25 mV) to the environment. Wounding and abrasion short-circuits this potential difference, leading to a standing voltage gradient from the intact epithelium into the wound site (the cathode) that directs epithelial cells and corneal nerves to migrate to fill the wound.[16,52] There is usually no overt wound during normal epithelial homeostasis, but persistent minor abrasion and cell loss could create a gradient of cumulative subacute wound load from the limbus to the center of the cornea, maintaining the electrical signal for cells and nerves to move centrally. We have recently shown that the barrier function of the $Pax6^{+/-}$ corneal epithelium is disrupted [54]; therefore, it seems unlikely that the mutants can maintain the epithelial potential difference. This may underlie the disrupted long distance cell migration and axon guidance in $Pax6^{+/-}$ corneal epithelia.

Why the Swirl?

Vortex formation has been observed and modeled mathematically in a cellular system (the chick epiblast), and though the formation of vortices may be initiated randomly, once formed they are mathematically impossible to eliminate.[55] The variation in orientation (clockwise or counterclockwise) in the vortex patterns observed in our system suggest that they are a stochastic consequence of minor targeting errors in the epithelial or growth cone centripetal movement. However, it is also possible that physical or other forces influence the formation of vortices, such as shearing forces exerted during blinking.[50] The vortex patterns we observed in wild-type corneal epithelia were consistent with a model whereby two discrete force vectors act on nerves and epithelial cells, a radial force directed centripetally and a tangential force directed perpendicularly to the direction of migration. Exposure to magnetic fields modulates directed cell growth in corneal epithelial cells, and a standing electric current that pushes epithelial cells toward the center of the cornea could elicit a concomitant magnetic field that may direct them sideways, explaining vortical patterns of cell migration.[56,57] It is possible that similar forces act on wild-type corneal epithelial nerves.

References

1. Hill RE, Favor J, Hogan BL, et al. Mouse small eye results from mutations in a paired-like homeobox-containing gene. *Nature.* 1991;354:522–525.
2. Grindley JC, Davidson DR, Hill RE. The role of Pax-6 in eye and nasal development. *Development.* 1995;121:1433–1442.
3. Koroma BM, Yang JM, Sundin OH. The Pax-6 homeobox gene is expressed throughout the corneal and conjunctival epithelia. *Invest Ophthalmol Vis Sci.* 1997;38:108–120.
4. Ramaesh T, Collinson JM, Ramaesh K, Kaufman MH, West JD, Dhillon B. Corneal abnormalities in $Pax6^{+/-}$ small eye mice mimic human aniridia-related keratopathy. *Invest Ophthalmol Vis Sci.* 2003;44:1871–1878.
5. Holland EJ, Djalilian AR, Schwartz GS. Management of aniridic keratopathy with keratolimbal allograft: a limbal stem cell transplantation technique. *Ophthalmology.* 2003;110:125–130.
6. Nishida K, Kinoshita S, Ohashi Y, Kuwayama Y, Yamamoto S. Ocular surface abnormalities in aniridia. *Am J Ophthalmol.* 1995; 120:368–375.
7. Hanson IM, Fletcher JM, Jordan T, et al. Mutations at the PAX6 locus are found in heterogeneous anterior segment malformations including Peters' anomaly. *Nat Genet.* 1994;6:168–173.
8. Ramaesh K, Ramaesh T, Dutton GN, Dhillon B. Evolving concepts on the pathogenic mechanisms of aniridia related keratopathy. *Int J Biochem Cell Biol.* 2005;37:547–557.
9. Baulmann DC, Ohlmann A, Flugel-Koch C, Goswami S, Cvekl A, Tamm ER. Pax6 heterozygous eyes show defects in chamber angle differentiation that are associated with a wide spectrum of other anterior eye segment abnormalities. *Mech Dev.* 2002;118:3–17.

10. Davis J, Duncan MK, Robison WG Jr, Piatigorsky J. Requirement for Pax6 in corneal morphogenesis: a role in adhesion. *J Cell Sci.* 2003;116:2157–2167.
11. Nelson LB, Spaeth GL, Nowinski TS, Margo CE, Jackson L. Aniridia: a review. *Surv Ophthalmol.* 1984;28:621–642.
12. Lazarov NE. Comparative analysis of the chemical neuroanatomy of the mammalian trigeminal ganglion and mesencephalic trigeminal nucleus. *Prog Neurobiol.* 2002;66:19–59.
13. Müller LJ, Marfurt CF, Kruse F, Tervo TM. Corneal nerves: structure, contents and function. *Exp Eye Res.* 2003;76:521–542.
14. Müller LJ, Vrensen GF, Pels L, Cardozo BN, Willekens B. Architecture of human corneal nerves. *Invest Ophthalmol Vis Sci.* 1997; 38:985–994.
15. Bee JA. The development and pattern of innervation of the avian cornea. *Dev Biol.* 1982;92:5–15.
16. Song B, Zhao M, Forrester J, McCaig C. Nerve regeneration and wound healing are stimulated and directed by an endogenous electrical field in vivo. *J Cell Sci.* 2004;117:4681–4690.
17. Baker KS, Anderson SC, Romanowski EG, Thoft RA, SundarRaj N. Trigeminal ganglion neurons affect corneal epithelial phenotype: influence on type VII collagen expression in vitro. *Invest Ophthalmol Vis Sci.* 1993;34:137–144.
18. Garcia-Hirschfeld J, Lopez-Briones LG, Belmonte C. Neurotrophic influences on corneal epithelial cells. *Exp Eye Res.* 1994;59:597–605.
19. Reid TW, Murphy CJ, Iwahashi CK, Foster BA, Mannis MJ. Stimulation of epithelial cell growth by the neuropeptide substance P. *J Cell Biochem.* 1993;52:476–485.
20. Nagano T, Nakamura M, Nakata K, et al. Effects of substance P and IGF-1 in corneal epithelial barrier function and wound healing in a rat model of neurotrophic keratopathy. *Invest Ophthalmol Vis Sci.* 2003;44:3810–3815.
21. Nakamura M, Kawahara M, Morishige N, Chikama T, Nakata K, Nishida T. Promotion of corneal epithelial wound healing in diabetic rats by the combination of a substance P-derived peptide (FGLM-NH2) and insulin-like growth factor-1. *Diabetologia.* 2003; 46:839–842.
22. Nakamura M, Kawahara M, Nakata K, Nishida T. Restoration of corneal epithelial barrier function and wound healing by substance P and IGF-1 in rats with capsaicin-induced neurotrophic keratopathy. *Invest Ophthalmol Vis Sci.* 2003;44:2937–2940.
23. Nakamura M, Ofuji K, Chikama T, Nishida T. Combined effects of substance P and insulin-like growth factor-1 on corneal epithelial wound closure of rabbit in vivo. *Curr Eye Res.* 1997;16:275–278.
24. Kruse FE, Tseng SC. Growth factors modulate clonal growth and differentiation of cultured rabbit limbal and corneal epithelium. *Invest Ophthalmol Vis Sci.* 1993;34:1963–1976.
25. Murphy CJ, Marfurt CF, McDermott A, et al. Spontaneous chronic corneal epithelial defects (SCCED) in dogs: clinical features, innervation, and effect of topical SP, with or without IGF-1. *Invest Ophthalmol Vis Sci.* 2001;42:2252–2261.
26. Woo HM, Bentley E, Campbell SF, Marfurt CF, Murphy CJ. Nerve growth factor and corneal wound healing in dogs. *Exp Eye Res.* 2005;80:633–642.
27. You L, Ebner S, Kruse FE. Glial cell-derived neurotrophic factor (GDNF)-induced migration and signal transduction in corneal epithelial cells. *Invest Ophthalmol Vis Sci.* 2001;42:2496–2504.
28. Davis EA, Dohlman CH. Neurotrophic keratitis. *Int Ophthalmol Clin.* 2001;41:1–11.
29. Benitez-del-Castillo JM, del Rio T, Iradier T, Hernandez JL, Castillo A, Garcia-Sanchez J. Decrease in tear secretion and corneal sensitivity after laser in situ keratomileusis. *Cornea.* 2001;20:30–32.
30. Patel SV, McLaren JW, Hodge DO, Bourne WM. Confocal microscopy in vivo in corneas of long-term contact lens wearers. *Invest Ophthalmol Vis Sci.* 2002;43:995–1003.
31. Wilson SE, Ambrosio R. Laser in situ keratomileusis-induced neurotrophic epitheliopathy. *Am J Ophthalmol.* 2001;132:405–406.
32. Schedl A, Ross A, Lee M, et al. Influence of PAX6 gene dosage on development: overexpression causes severe eye abnormalities. *Cell.* 1996;86:71–82.
33. Tan SS, Williams EA, Tam PP. X-chromosome inactivation occurs at different times in different tissues of the post-implantation mouse embryo. *Nat Genet.* 1993;3:170–174.
34. Collinson JM, Chanas SA, Hill RE, West JD. Corneal development, limbal stem cell function, and corneal epithelial cell migration in the Pax6$^{+/-}$ mouse. *Invest Ophthalmol Vis Sci.* 2004;45:1101–1108.
35. Collinson JM, Morris L, Reid AI, et al. Clonal analysis of patterns of growth, stem cell activity, and cell movement during the development and maintenance of the murine corneal epithelium. *Dev Dyn.* 2002;224:432–440.
36. Dorà NJ, Kucerova R, Parisi I, West JD, Collinson JM. Pax6 dosage effects on corneal development, growth and wound healing. *Dev Dyn.* 2008;237:1295–1306.
37. Yu CQ, Rosenblatt MI. Transgenic corneal neurofluorescence in mice: a new model for in vivo investigation of nerve structure and regeneration. *Invest Ophthalmol Vis Sci.* 2007;48:1535–1542.
38. van Raamsdonk CD, Tilghman SM. Dosage requirement and allelic expression of PAX6 during lens placode formation. *Development.* 2000;127:5439–5448.
39. Quinn JC, West JD, Kaufman MH. Genetic background effects on dental and other craniofacial abnormalities in homozygous small eye Pax6^{Sey}/Pax6^{Sey} mice. *Anat Embryol (Berl).* 1997;196:311–321.
40. Collinson JM, Quinn JC, Buchanan MA, et al. Primary defects in the lens underlie complex anterior segment abnormalities of the Pax6 heterozygous eye. *Proc Natl Acad Sci U S A.* 2001;98:9688–9693.
41. Chan KY, Haschke RH. Action of a trophic factor(s) from rabbit corneal epithelial culture on dissociated trigeminal neurons. *J Neurosci.* 1981;1:1155–1162.
42. Chan KY, Haschke RH. Isolation and culture of corneal cells and their interactions with dissociated trigeminal neurons. *Exp Eye Res.* 1982;35:137–156.
43. Forbes DJ, Pozos RS, Nelson JD. Co-culture of rat trigeminal ganglion neurons and corneal epithelium. *Curr Eye Res.* 1987;6:507–514.
44. Ogilvy CS, Silverberg KR, Borges LF. Sprouting of corneal sensory fibers in rats treated at birth with capsaicin. *Invest Ophthalmol Vis Sci.* 1991;32:112–121.
45. Cotsarelis G, Cheng SZ, Dong G, Sun TT, Lavker RM. Existence of slow-cycling limbal epithelial basal cells that can be preferentially stimulated to proliferate: implications on epithelial stem cells. *Cell.* 1989;57:201–209.
46. Burbach GJ, Kim KH, Zivony AS, et al. The neurosensory tachykinins substance P and neurokinin A directly induce keratinocyte nerve growth factor. *J Invest Dermatol.* 2001;117:1075–1082.
47. Leiper LJ, Walczysko P, Kucerova R, et al. The roles of calcium signaling and ERK1/2 phosphorylation in a *Pax6*$^{+/-}$ mouse model of epithelial wound-healing delay. *BMC Biol.* 2006;4:27.
48. Nagasaki T, Zhao J. Centripetal movement of corneal epithelial cells in the normal adult mouse. *Invest Ophthalmol Vis Sci.* 2003; 44:558–566.
49. Dvorscak L, Marfurt CF. Age-related changes in rat corneal epithelial nerve density. *Invest Ophthalmol Vis Sci.* 2008;49:910–916.
50. Patel DV, McGhee CN. Mapping of the normal human corneal sub-basal nerve plexus by in vivo laser scanning confocal microscopy. *Invest Ophthalmol Vis Sci.* 2005;46:4485–4488.
51. Patel DV, McGhee CN. Mapping the corneal sub-basal nerve plexus in keratoconus by in vivo laser scanning confocal microscopy. *Invest Ophthalmol Vis Sci.* 2006;47:1348–1351.
52. McCaig CD, Rajnicek AM, Song B, Zhao M. Controlling cell behavior electrically: current views and future potential. *Physiol Rev.* 2005;85:943–978.
53. Zhao M, Song B, Pu J, et al. Electrical signals control wound healing through phosphatidylinositol-3-OH kinase-gamma and PTEN. *Nature.* 2006;442:457–460.
54. Ou J, Walczysko P, Kucerova R, et al. Chronic wound state exacerbated by oxidative stress in *Pax6*$^{+/-}$ aniridia-related keratopathy. *J Pathol.* 2008;215:421–430.
55. Newman T. Grid-free models of multicellular systems, with an application to large-scale vortices accompanying primitive streak formation. *Curr Topics Dev Biol.* 2008;81:157–182.
56. Dua HS, Singh A, Gomes JA, Laibson PR, Donoso LA, Tyagi S. Vortex or whorl formation of cultured human corneal epithelial cells induced by magnetic fields. *Eye.* 1996;10:447–450.
57. Dua HS, Watson NJ, Mathur RM, Forrester JV. Corneal epithelial cell migration in humans: "hurricane and blizzard keratopathy." *Eye.* 1993;7:53–58.